Journal of Sound and Vibration (2001) **248**(4), 745–761
doi:10.1006/jsvi.2001.3828, available online at http://www.idealibrary.com on IDEAL®

FULLY COMPUTERIZED APPROACH TO STUDY CABLE-STAYED BRIDGE–VEHICLE INTERACTION

W. H. Guo and Y. L. Xu

Department of Civil and Structural Engineering, The Hong Kong Polytechnic University, Hung Hom, Kowloon, Hong Kong. E-mail: ceylxu@polyu.edu.hk

(*Received* 7 *September* 2000, *and in final form* 12 *June* 2001)

This paper presents a fully computerized approach for assembling equations of motion of any types of coupled vehicle–bridge systems. Heavy road vehicles are idealized as a combination of a number of rigid bodies connected by a series of springs and dampers while the bridge is modelled using the conventional finite element method. The mass matrix, stiffness matrix, damping matrix, and force vector of coupled vehicle–bridge systems are automatically assembled using the fully computerized approach and taking into account road surface roughness. The required input data about vehicles to the computer program are only the dynamic properties and the positions of rigid bodies, springs, and dampers, and constraint conditions. The derived equations of motion of the coupled vehicle–bridge system are then solved by the direct integration method. A case study of a real long span cable-stayed bridge with a group of moving heavy vehicles demonstrates that the fully computerized approach and the associated computer program provide an efficient and convenient tool for studying the interaction problems of large complicated bridges with various types of running vehicles.

1. INTRODUCTION

Dynamic vehicle–bridge interaction problems have been studied by many investigators since the middle of 19th century [1–5]. Because of the limitation of computation capacity in the early stage, only simplified models of vehicle–bridge systems could be considered. For instance, a moving vehicle was modelled as a moving load without considering the effect of inertia force [6], and later a moving-mass model was used instead of a moving load to include inertia force effects [1]. Nowadays, the volume of traffic and the speed of vehicles have increased considerably, and the configurations of vehicles have also changed dramatically. More sophisticated and rational models and computerized approaches are thus needed.

To study three-dimensional vibration of coupled vehicle–bridge systems, the stiffness matrix, mass matrix, damping matrix, and force vector of both vehicles and bridge should be first formed. Then the contact points between the bridge deck and vehicles couple the two components together. Most previous investigators treated the problem using two sets of differential equations of motion, one for the bridge and the other for the vehicle, and then considering contact conditions through an iteration [7]. In the iteration, the displacements of the contact points are assumed first. The interaction forces between the vehicles and bridge are then calculated by solving the equations of motion of vehicles. The improved displacements of the contact points are obtained by solving the equations of motion of bridge using the calculated interaction forces. The iteration process will be finally terminated only if the displacements of all the contact points from the two consecutive iterations are close enough. The advantage of such an approach is that the dynamic

0022-460X/01/490745 + 17 $35.00/0

property matrices in the two sets of equations of motion remain constant. However, the convergence rate of the iteration is likely to be slow when the bridge is subjected to a series of vehicles in motion, for there exist too many contact points [8]. Also, the set of differential equations of motion for vehicles can be established only if the type of vehicle is specified. When the type of vehicle is changed, the equations of motion should be re-derived.

The other way is to solve the equations of motion of coupled vehicle–bridge system using the direct integration method and the solution is given at each time step without any iteration. The major disadvantage using this approach is that the equations of motion of the coupled system are time-dependent and at each time step the characteristic matrices in the equations of motion should be modified. To reduce the computation efforts required in this approach, the modal superposition method may be applied to the bridge [9]. The coupled vehicle–bridge system vectors contain the modal components for the bridge and the physical components for the vehicles, and as a result the degrees of freedom of the coupled system are significantly reduced. The major disadvantage of this approach is that the modal analysis to find the natural frequencies and mode shapes of the bridge is indispensable and the local deformation due to high frequencies may be difficult to be predicted.

A relatively new approach to the dynamic analysis of vehicle–bridge interaction is called the condensation method [10]. The major feature of this approach is that all the degrees of freedom of a vehicle are condensed to the associated bridge's degrees of freedom by using the Guyan reduction scheme or the dynamic condensation method. However, it is not easy to use this approach to determine the dynamic response of vehicle, which serves as an indicator of the driver and passenger comfort. Recently, Yang and Yau [8] used the Newmark's finite differential formulas to condense the sprung mass, which represents part of a vehicle, to those of the bridge such that the dynamic responses of the sprung masses can be determined together with those of the bridge. However, if the more realistic model of the vehicle is considered, it becomes difficult to derive the essential formulas by which the displacement increment of the vehicle can be expressed by the bridge displacements.

From the foregoing review, it is seen that most of the existing methods are not fully computerized to form the equations of motion of a bridge with different types of vehicles running over it. The types of vehicles on the bridge should be decided before the formulation. The cases in which a vehicle enters onto the bridge or leaves the bridge are difficult to be handled. Some of them also cannot efficiently compute the dynamic responses of both bridge and vehicles simultaneously and evaluate the serviceability performance of the vehicles. In this connection, this paper presents a fully computerized approach to form the equations of motion of coupled vehicle–bridge systems. The developed computer program can handle more realistic models of long span cable-stayed bridges under various types of moving vehicles. The effect of road surface roughness can be easily taken into consideration in the analysis. The situation in which a vehicle enters onto the bridge or leaves the bridge can be easily dealt with. However, the equations of motion formed using the suggested approach are also coupled and thus at each time step the characteristic matrices in the equations of motion of the coupled system should be modified. A real long span cable-stayed bridge under a group of moving heavy road vehicles is selected as a case study to demonstrate the advantage of the proposed approach and the associated computer program.

2. MODELLING OF VEHICLE AND BRIDGE

2.1. MODELLING OF VEHICLE

There are a variety of configurations of vehicles in reality, including the tractor with trailers having different axle spacings. In this study, a vehicle is modelled as a combination

of several rigid bodies connected by a series of springs, damping devices, and pivots. The co-ordinate system for the vehicle is the same as the co-ordinate system for the bridge (see Figures 1 and 3). The X-, Y-, and Z-axis are set in the longitudinal, lateral, and vertical directions of the bridge, respectively, following a right-hand rule.

The rigid bodies can be used to represent vehicle bodies, the axles, the wheels, or others. The centre of gravity of each rigid body is taken as a node. In a most general case, a node has six degrees of freedom: three translational degrees and three rotational degrees. The corresponding displacements and rotations are assumed to remain small throughout the analysis so that the sines of the angles of rotation may be taken equal to angles themselves and the cosines of the angles of rotation may be taken as unity. The mass and/or the mass moments of inertia of each rigid body are calculated from the weight distribution and dimension of the body with respect to the local co-ordinate originated at its node.

The contact between the bridge deck and the moving tyre of the vehicle is assumed to be a point contact. With the assumption that the road surface profile is not too rough to make the vehicle jump or leave the riding surface, the tyres of the vehicle remain in contact with the bridge deck at all times. No matter whether the mass of the tyre is lumped at the contact point or not, the vertical displacement of the tyre is not an independent degree of freedom, and actually it can be expressed in terms of the relevant degrees of freedom of the bridge and the road surface profile.

The springs can be used to model the suspension system, the flexibility of a tyre, or others. Each spring is assumed to be massless. Besides the stiffness coefficient of each spring, the positions of the two ends of the spring connecting two rigid bodies or connecting one rigid body and one contact point are required as input data. The energy dissipation capacity of the suspension system, the tyre, or others can be modelled by damping devices. If the damping device is of the viscous type, the damping coefficient can be used as a sole parameter for the damping device. The positions of the two ends of the damping device connecting two rigid bodies or one rigid body and one contact point should also be identified as input data. The pivots may be used to connect the trailer to the tractor, for which the constraint equations will be correspondingly developed.

In summary, the independent degrees of freedom of a vehicle in the coupled vehicle–bridge system are the sum of the degrees of freedom of all the rigid bodies, excluding the masses at the contact points in the vertical direction, minus the number of the constraint equations. The required input data about vehicles to the computer program at a given time are the dynamic properties and positions of all the rigid bodies and springs and damping devices, the positions of all the contact points, and the constraint conditions for all the pivots. Based on these input data, the mass matrix, damping matrix, and stiffness matrix of the vehicle itself and the coupled mass, damping, and stiffness matrices and the contact force vectors of the vehicle with the bridge can be automatically assembled using the fully computerized approach, which will be explained in detail in the following sections.

2.2. MODELLING OF BRIDGE

A long span cable-supported bridge model can be established using different types of finite elements such as beam element, cable element, plate element, and solid element [11]. The stiffness matrix and mass matrix and force vector of the bridge can be obtained using the conventional finite element method. The structural damping of the bridge is assumed to be Rayleigh damping. The damping matrix of the bridge can be thus expressed as the function of the mass and stiffness matrices.

$$[C_b] = \alpha_b [M_b] + \beta_b [K_b], \tag{1}$$

where $[M_b]$, $[C_b]$ and $[K_b]$ are the mass matrix, damping matrix and stiffness matrix of the bridge, respectively; and α_b and β_b are the Rayleigh damping factors which can be evaluated if the two structural damping ratios associated with the two specific frequencies are known. The equations of motion of the bridge alone without moving vehicles can be expressed as

$$[M_b]\{\ddot{v}_b\} + [C_b]\{\dot{v}_b\} + [K_b]\{v_b\} = \{P_{be}\}, \tag{2}$$

where $\{v_b\}$, $\{\dot{v}_b\}$, and $\{\ddot{v}_b\}$ are the nodal dynamic displacement, velocity, and acceleration vectors of the bridge, respectively; and $\{P_{be}\}$ is the external force vector of the bridge.

2.3. MODELLING OF ROAD SURFACE ROUGHNESS

Many investigations have shown that the roughness of the bridge surface is an important factor that affects the dynamic responses of both the bridge and vehicle [12]. The road surface roughness may be described as a realization of a random process that can be described by a power spectral density (PSD) function. The following PSD functions were proposed by Dodds and Robson [13] for highway road surface roughness:

$$S(\bar{\phi}) = A_r\left(\frac{\bar{\phi}}{\bar{\phi}_0}\right)^{-w_1}, \quad \bar{\phi} \leqslant \bar{\phi}_0, \tag{3}$$

$$S(\bar{\phi}) = A_r\left(\frac{\bar{\phi}}{\bar{\phi}_0}\right)^{-w_2}, \quad \bar{\phi} \geqslant \bar{\phi}_0, \tag{4}$$

where $S(\bar{\phi})$ is the PSD function (m^3/cycle) for the road surface elevation; $\bar{\phi}$ is the spatial frequency (cycle/m); $\bar{\phi}_0$ is the discontinuity frequency of $1/2\pi$ (cycle/m); and A_r is the roughness coefficient (m^3/cycle) and its value depends on the road condition. The power exponents w_1 and w_2 vary from 1·36 to 2·28 [13]. To simplify the description of the road surface roughness, Huang and Wang [14] suggested the following PSD function:

$$S(\bar{\phi}) = A_r\left(\frac{\bar{\phi}}{\bar{\phi}_0}\right)^{-2}. \tag{5}$$

The road surface roughness is assumed to be a zero-mean stationary Gaussian random process. Therefore, it can be generated through an inverse Fourier transform.

$$r(x) = \sum_{k=1}^{N} \sqrt{2S(\bar{\phi}_k)\,\Delta\bar{\phi}}\cos(2\pi\bar{\phi}_k x + \theta_k), \tag{6}$$

where θ_k is the random phase angle uniformly distributed from 0 to 2π.

3. COMPUTERIZED ASSEMBLAGE OF EQUATIONS OF MOTION

In most of the previous studies, the equations of motion of a vehicle are derived by hand using either D'Alembert's principle or the principle of virtual work or the Hamilton's principle. The derived equations of motion of the vehicle are then combined with the equations of motion of the bridge. However, for a long span cable-supported bridge with a group of moving vehicles of various configurations, it may not be easy to assemble the equations of motion of the coupled vehicle–bridge systems in this way. In this study,

a computerized approach is suggested to expand the equations of motion of the bridge, obtained by the finite element method, to the equations of motion of the coupled vehicle–bridge systems. The computerized approach uses the principle of virtual work to fulfil such a task.

3.1. PRINCIPLE OF COMPUTERIZED APPROACH

Assume that the coupled vehicle and bridge system has N independent degrees of freedom denoted by the displacement vector $\{v\}$, in which the degrees of freedom of the vehicle are N_v with the displacement vector $\{v_v\}$ and the degrees of freedom of the bridge are $N_b = N - N_v$ with the displacement vector $\{v_b\}$. The virtual displacement vectors can be then expressed as $\{\delta v\}$, $\{\delta v_v\}$, and $\{\delta v_b\}$ for the coupled system, the vehicle, and the bridge, respectively, and the external force vectors can be expressed as $\{P\}$, $\{P_v\}$, and $\{P_b\}$ accordingly. In the computerized approach, the following steps are taken to expand the equations of motion of the bridge alone to the equations of motion of the coupled vehicle–bridge system.

- Express the relative displacement of each spring in the vehicle as the function of the displacement vector $\{v\}$. Express the relative velocity of each viscous damper as the function of the velocity vector $\{\dot{v}\}$. For the spring connecting two rigid bodies of the vehicle, this can be done by relating the given positions of the two ends of the spring to the displacements of the two rigid bodies, which may require considering the constraint conditions. For the spring connecting one rigid body and one contact point, the road surface profile and the relevant displacements of the bridge are involved. A similar way is used to handle the viscous dampers.
- Compute all the inertia forces, the elastic forces, and the damping forces acting on the vehicle based on the given spring stiffness and damper damping coefficients, the computed mass and mass moment of inertia, and the computed relative displacements and velocities. This will lead to many terms and each term falls into one of the four categories: $C_m\ddot{v}_j$, $C_c\dot{v}_j$, $C_k v_j$, and P_r, where P_r is the force due to the road surface roughness and $1 \leqslant j \leqslant N$.
- Compute the virtual work done by all the forces on each virtual displacement. This will again produce many terms and each term falls into one of the four categories: $\delta v_i C_m \ddot{v}_j$, $\delta v_i C_c \dot{v}_j$, $\delta v_i C_k v_j$, and $\delta v_i P_r$, where $1 \leqslant i, j \leqslant N$.
- Identify the mass or mass moment coefficients, the stiffness coefficients, the damping coefficients, and the force components and put them into the proper positions of the system mass matrix, damping matrix, stiffness matrix, and force vector. For instance, the term $\delta v_i C_m \ddot{v}_j$ indicates that C_m should be added to the mass coefficient m_{ij} at the ith row and jth column of the system mass matrix. In a similar way, C_c in the term $\delta v_i C_c \dot{v}_j$ and C_k in the term $\delta v_i C_k v_j$ should be added to the damping coefficient c_{ij} at the ith row and jth column of the system damping matrix and the stiffness coefficient k_{ij} at the ith row and jth column of the system stiffness matrix respectively. The term $\delta v_i P_r$ indicates that the force P_r should be added to the ith force coefficient P_i of the system force vector.

It should be pointed out that since the virtual work is scalar quantity and the total virtual work of the vehicle done by all the forces can be determined by the algebraic summation of the virtual work done by each force, the coefficient in each system matrix can be assembled algebraically. This approach is particularly suitable for the expansion of equations of motion of the bridge to the equations of motion of the coupled vehicle and bridge system. The advantages of this approach will be demonstrated in the case study.

3.2. EQUATIONS OF MOTION OF COUPLED VEHICLE–BRIDGE SYSTEM

The use of the fully computerized approach can easily lead to the following equations of motion of the coupled bridge and vehicle system, established from the static equilibrium position of the system.

$$\begin{bmatrix} M_b + M_{bbv} & 0 \\ 0 & M_v \end{bmatrix} \begin{Bmatrix} \ddot{v}_b \\ \ddot{v}_v \end{Bmatrix} + \begin{bmatrix} C_b + C_{bbv} & C_{bv} \\ C_{vb} & C_{v1} + C_{v2} \end{bmatrix} \begin{Bmatrix} \dot{v}_b \\ \dot{v}_v \end{Bmatrix}$$

$$+ \begin{bmatrix} K_b + K_{bbv} & K_{bv} \\ K_{vb} & K_{v1} + K_{v2} \end{bmatrix} \begin{Bmatrix} v_b \\ v_v \end{Bmatrix} = \begin{Bmatrix} P_{bvg} + P_{bvr1} + P_{bvr2} + P_{bvr3} \\ P_{vvr2} + P_{vvr3} \end{Bmatrix}. \tag{7}$$

In equation (7), $[M_b]$, $[C_b]$, and $[K_b]$ are the mass matrix, damping matrix, and stiffness matrix of the bridge alone, respectively, obtained by the conventional finite element method. The matrix $[M_{bbv}]$ is related to the inertia forces of all the masses of the vehicle at the contact points due to the bridge accelerations while the matrix $[M_v]$ corresponds to the inertia forces of all the rigid bodies of the vehicle, excluding the masses at the contact points. The inertia forces of all the masses of the vehicle at the contact points due to the road surface roughness constitute the force vector $\{P_{bvr1}\}$. For the dampers whose relative velocities are a function of the degrees of freedom of the vehicle only, the damper forces lead to the matrix $[C_{v1}]$. For the dampers connected to the contact points, their relative velocities depend on not only the degrees of freedom of the vehicle but also on the degrees of freedom of the bridge and the road surface roughness. As a result, the coupled damping matrices $[C_{bv}]$ and $[C_{vb}]$, the additional damping matrix $[C_{bbv}]$ to the bridge damping matrix $[C_b]$, the additional damping matrix $[C_{v2}]$ to the vehicle damping matrix $[C_{v1}]$, the additional force vector on the bridge $\{P_{bvr2}\}$ due to the road surface roughness, and the additional force vector on the vehicle $\{P_{vvr2}\}$ due to the road surface roughness are generated. Similarly, for the springs whose relative displacements are a function of the degrees of freedom of the vehicle only, the spring forces lead to the matrix $[K_{v1}]$. From the springs connected to the contact points, the stiffness matrices $[K_{bv}]$, $[K_{vb}]$, $[K_{bbv}]$, $[K_{v2}]$ and the additional force vectors due to road surface roughness $\{P_{bvr3}\}$ and $\{P_{vvr3}\}$ are constituted. The last but not least is the external forces on the bridge due to the gravity forces of the vehicle denoted by the force vector $\{P_{bvg}\}$.

4. CASE STUDY

To make sure that the suggested fully computerized approach and the associated computer program work properly and accurately, the responses of one simply supported beam under moving load and one simply supported beam under moving sprung mass were computed respectively [15]. The results were compared with the existing analytical solutions and those obtained by other researchers using other approaches. The comparison was found very satisfactory. The more complicated case study taking a real long span cable-stayed bridge under a group of moving heavy road vehicles is presented in this paper. The implementation of the computerized approach is also demonstrated to make the approach easy to understand.

4.1. CABLE-STAYED BRIDGE

The concerned triple-tower cable-stayed bridge has an overall length of 1177 m with the two main spans measured at 475 and 448 m and the two side spans of 127 m each (see

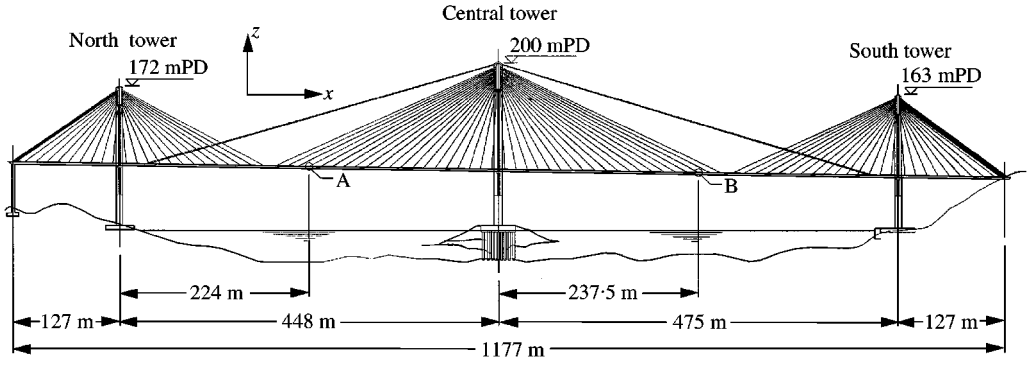

Figure 1. Configuration of long span cable-stayed bridge used in case study.

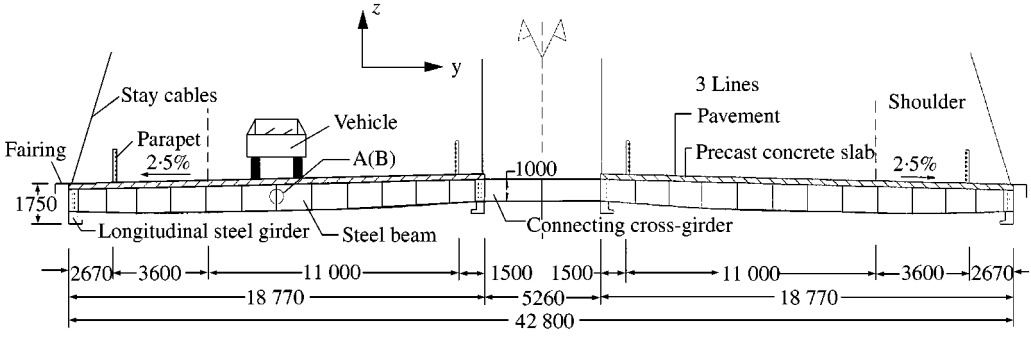

Figure 2. Typical deck cross-section of bridge.

Figure 1). The three bridge towers are all single leg concrete towers. The central tower reaches a height of 200 m above sea level with the end towers having heights of 163 and 172 m above sea level respectively. Two large steel tower heads, each weighing some 170 t, are installed at the top of each tower from which 384 stay cables in four planes radiate downwards to support the bridge deck at 13·5 m intervals. The towers are stabilized by transverse cables running from the tower head to the cross struts and section of tower below deck level. The central tower is further stabilized longitudinally with two longitudinal stay cables. The bridge deck is separated into two carriageway structures and each carriageway structure is formed by two longitudinal steel plate girders with steel beams spanning transversely between them at 4·5 m centres (see Figure 2). The cross-girders are extended at 13·5 m intervals to link the two separated carriageway structures.

A three-dimensional dynamic finite element model is established for the triple-tower cable-stayed bridge. Three-dimensional Timoshenko beam elements are used to model the three bridge towers. The stay cables and stabilizing cables are modelled by cable elements accounting for geometric non-linearity due to cable tension. Each carriageway structure is represented by a three-girder model consisting of one central girder and two side girders connected by transverse links [16]. All the girders are modelled by the three-dimensional Timoshenko beam elements. The connections between bridge components and the supports of the bridge are also properly modelled. The modal analysis of the bridge shows that the natural frequencies of the bridge are spaced very closely. The fundamental frequencies in the lateral, vertical, and torsional directions are 0·216, 0·189, and 0·387 Hz respectively. In the analysis of the bridge–vehicle interaction, the damping ratios of the bridge are taken as 1%.

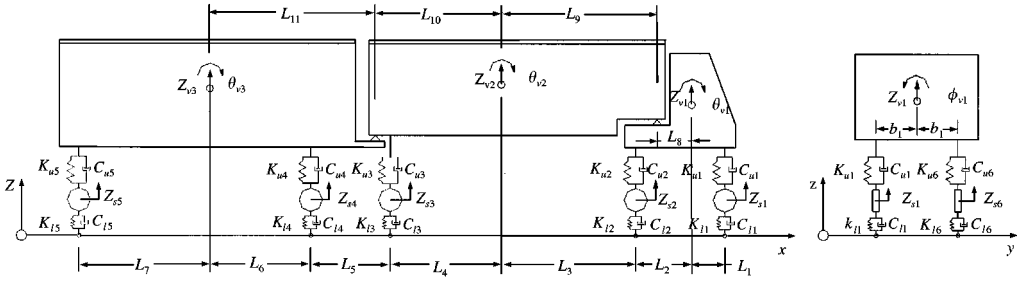

Figure 3. Tractor–trailer model.

4.2. TRACTOR–TRAILER VEHICLE

Heavy tractor–trailer vehicles that frequently run on the cable-stayed bridge are taken as example vehicles in this study. The vehicle model comprises 13 rigid bodies: one for tractor, two for two trailers, and 10 for five axle sets including weights of tyres and brakes (see Figure 3). The suspension system at each axle set, connecting the axle to either the tractor or trailer, is represented by the two identical units across the width of the vehicle. Each unit is a parallel combination of a linear elastic spring of stiffness K_{ui} and a viscous damper of damping coefficient C_{ui}. The parallel combination of a linear elastic spring of stiffness K_{li} and a viscous damper of damping coefficient C_{li} is used to represent the dynamic characteristics of the tyre. There are also two identical units connecting each axle to the bridge deck. The horizontal distance between the two units is $2b_1$. If only the vertical vibration of the vehicle is considered in the analysis, the rigid bodies representing either the tractor or trailers are each assigned three degrees of freedom: the vertical displacement (Z_{vi}), the rotation about the transverse axis (pitch θ_{vi}), and the rotation about the longitudinal axis (roll ϕ_{vi}). The rigid body representing the axle set is assigned only one degree of freedom in the vertical direction (Z_{sli}, or Z_{sri}). Since the tractor and trailer are connected by a frictionless pivot and the two trailers are also connected by a frictionless pivot, the two constraint equations should be introduced. The total degrees of freedom of the vehicle are not 19 but only 17. The main parameters of the vehicle are listed in Table 1 [17]. The first natural frequency of the vehicle is about 3·21 Hz in the vertical direction.

4.3. COMPUTERIZED ASSEMBLAGE OF EQUATIONS OF MOTION

By using the conventional finite element approach, the mass matrix $[M_b]$, the damping matrix $[C_b]$, and the stiffness matrix $[K_b]$ of the bridge alone can be easily assembled. Then, expand the displacement vector of the bridge $\{v_b\}$to include the displacement vector of the vehicle $\{v_v\}$.

$$\{v_v\} = \{Z_{v1}\ \theta_{v1}\ \phi_{v1}\ Z_{v2}\ \phi_{v2}\ Z_{v3}\ \phi_{v3}\ Z_{sl1}\ Z_{sl2}\ Z_{sl3}\ Z_{sl4}\ Z_{sl5}\ Z_{sr1}\ Z_{sr2}\ Z_{sr3}\ Z_{sr4}\ Z_{sr5}\}, \quad (8)$$

where Z_{v1}, Z_{v2} and Z_{v3} are the vertical displacements of the tractor and two trailers, respectively, at its own centroid measured from the position of static equilibrium; θ_{v1} is the rotation about the transverse axis of the tractor; ϕ_{v1}, ϕ_{v2} and ϕ_{v3} denote the rotations about the longitudinal axis of the tractor and two trailers, respectively; Z_{sli} and Z_{sri} $(i = 1, 2, \ldots, 5)$ are left and right vertical displacements of the five axle sets, respectively, at its own centroid measured from the position of static equilibrium. Clearly, the above 17 displacements are independent.

TABLE 1

Main parameters of vehicles used in case study

Parameter	Unit	Value
Full length of vehicle (L)	m	16·0
Total weight of vehicle (W_v)	kN	682·53
Mass of tractor (M_{v1})	kg	9060
Pitching moment of inertia of tractor (J_{yv1})	kg m^2	17 395
Rolling moment of inertia of tractor (J_{xv1})	kg m^2	3020
Mass of the first trailer (M_{v2})	kg	29 006
Pitching moment of inertia of the first trailer (J_{yv2})	kg m^2	29 219
Rolling moment of inertia of the first trailer (J_{xv2})	kg m^2	9669
Mass of the second trailer (M_{v3})	kg	24460
Pitching moment of inertia of the second trailer (J_{yv3})	kg m^2	53 462
Rolling moment of inertia of the second trailer (J_{xv3})	kg m^2	8153
Mass of axle set ($M_{s1} = M_{s4} = M_{s6} = M_{s9}$)	kg	445
Upper spring stiffness ($K_{u1} = K_{u4} = K_{u6} = K_{u9}$)	kN/m	4000
Upper damper damping coefficient ($C_{u1} = C_{u4} = C_{u6} = C_{u9}$)	kN s/m	20
Mass of axle set ($M_{s2} = M_{s3} = M_{s5} = M_{s7} = M_{s8} = M_{s10}$)	kg	890
Upper spring stiffness ($K_{u2} = K_{u3} = K_{u5} = K_{u7} = K_{u8} = K_{u10}$)	kN/m	8000
Upper damper damping coefficient ($C_{u2} = C_{u3} = C_{u5} = C_{u7} = C_{u8} = C_{u10}$)	kN s/m	20
Lower spring stiffness ($K_{l1} = K_{l4} = K_{l6} = K_{l9}$)	kN/m	2250
Lower damper damping coefficient ($C_{l1} = C_{l4} = C_{l6} = C_{l9}$)	kN s/m	20
Lower spring stiffness ($K_{l2} = K_{l3} = K_{l5} = K_{l7} = K_{l8} = K_{l10}$)	kN/m	8000
Lower damper damping coefficient ($C_{l2} = C_{l3} = C_{l5} = C_{l7} = C_{l8} = C_{l10}$)	kN s/m	20
Distance (L_1)	m	1·6
Distance (L_2)	m	2·4
Distance (L_3)	m	1·64
Distance (L_4)	m	3·36
Distance (L_5)	m	2·0
Distance (L_6)	m	3·055
Distance (L_7)	m	1·945
Distance (L_8)	m	2·4
Distance (L_9)	m	1·64
Distance (L_{10})	m	3·36
Distance (L_{11})	m	5·055
Distance (b_1)	m	0·9575

To expand the mass matrix, damping matrix, stiffness matrix and force vector of the bridge to those of the coupled bridge–vehicle systems, the inertial forces and damping forces and elastic forces of the vehicle should be computed. Since there is no mass at the contact point, it is very easy to determine the inertial forces acting on the rigid bodies. To determine the elastic forces and damping forces, the relative displacement of each spring and the relative velocity of each damper should be computed based on the given geometric information and sign convention. For instance, the deformations of the upper springs can be expressed as

$$\Delta_{ul1} = Z_{v1} - L_1\theta_{v1} - b_1\phi_{v1} - Z_{sl1}, \qquad \Delta_{ur1} = Z_{v1} - L_1\theta_{v1} + b_1\phi_{v1} - Z_{sr1}, \tag{9, 10}$$

$$\Delta_{ul2} = Z_{v1} + L_2\theta_{v1} - b_1\phi_{v1} - Z_{sl2}, \qquad \Delta_{ur2} = Z_{v1} + L_2\theta_{v1} + b_1\phi_{v1} - Z_{sr2}, \tag{11, 12}$$

$$\Delta_{ul3} = Z_{v2} + L_4\theta_{v2} - b_1\phi_{v2} - Z_{sl3}, \qquad \Delta_{ur3} = Z_{v2} + L_4\theta_{v2} + b_1\phi_{v2} - Z_{sr3}, \tag{13, 14}$$

$$\Delta_{ul4} = Z_{v3} - L_6\theta_{v3} - b_1\phi_{v3} - Z_{sl4}, \qquad \Delta_{ur4} = Z_{v3} - L_6\theta_{v3} + b_1\phi_{v3} - Z_{sr4}, \quad (15, 16)$$

$$\Delta_{ul5} = Z_{v3} + L_7\theta_{v3} - b_1\phi_{v3} - Z_{sl5}, \qquad \Delta_{ur5} = Z_{v3} + L_7\theta_{v3} + b_1\phi_{v3} - Z_{sr5}, \quad (17, 18)$$

where Δ_{uli} and Δ_{uri} $(i = 1, 2, \ldots, 5)$ are the deformations of the upper left and right springs at the five axle sets respectively. The two constraint conditions can be expressed as

$$Z_{v1} + L_8\theta_{v1} = Z_{v2} - L_9\theta_{v2}, \qquad Z_{v2} + L_{10}\theta_{v2} = Z_{v3} - L_{11}\theta_{v3}. \quad (19, 20)$$

Thus, θ_{v2} and θ_{v3} can be expressed in terms of the independent degrees of freedom of the vehicle.

$$\theta_{v2} = \frac{Z_{v2} - Z_{v1} - L_8\theta_{v1}}{L_9}, \quad (21)$$

$$\theta_{v3} = \frac{L_9 Z_{v3} - (L_9 + L_{10})Z_{v2} + L_{10}Z_{v1} + L_8 L_{10}\theta_{v1}}{L_9 L_{11}}. \quad (22)$$

Accordingly, the deformations of all the upper springs (see equations (9)–(18)) can be expressed in terms of the independent degrees of freedom of the vehicle only. The deformations of the lower springs are

$$\Delta_{lli} = Z_{sli} - Z_{li} \quad (i = 1, 2, \ldots, 5), \quad (23)$$

$$\Delta_{lri} = Z_{sri} - Z_{ri} \quad (i = 1, 2, \ldots, 5), \quad (24)$$

where Δ_{lli} and Δ_{lri} $(i = 1, 2, \ldots, 5)$ are the deformations of the lower left and right springs at the five axle sets, respectively; and Z_{li} and Z_{ri} $(i = 1, 2, \ldots, 5)$ denote the vertical displacements of the left contact point and right contact point respectively. If the ith left and right tyres of the vehicle run on the bridge, the vertical displacement of the ith contact point can be expressed in terms of the relevant degrees of freedom of the bridge and the road surface roughness as follows:

$$Z_{li} = N_{li}(x)\{\delta\}_{bi}^{e} + r_{li}(x), \qquad Z_{ri} = N_{ri}(x)\{\delta\}_{bi}^{e} + r_{ri}(x), \quad (25, 26)$$

in which r_{li} and r_{ri} are the road surface roughness under the ith left and right contact points, respectively; $\{\delta\}_{bi}^{e}$ is the displacement vector of the bridge element over which the ith contact point runs and it is also the subset of the displacement vector of the bridge $\{v_b\}$; and N_{li} is the transfer function from the node displacements of the bridge element to the displacement of the ith left contact point. The velocity and acceleration of the ith left contact point are computed by

$$\dot{Z}_{li} = N_{li}(x)\{\dot{\delta}\}_{bi}^{e} + u\frac{\partial N_{li}(x)}{\partial x}\{\delta\}_{bi}^{e} + \frac{\partial r_{li}(x)}{\partial x}u, \quad (27)$$

$$\ddot{Z}_{li} = N_{li}(x)\{\ddot{\delta}\}_{bi}^{e} + 2u\frac{\partial N_{li}(x)}{\partial x}\{\dot{\delta}\}_{bi}^{e} + u^2\frac{\partial^2 N_{li}(x)}{\partial x^2}\{\delta\}_{bi}^{e} + a\frac{\partial N_{li}(x)}{\partial x}\{\delta\}_{bi}^{e} + \frac{\partial r_{li}(x)}{\partial x}a + \frac{\partial^2 r_{li}(x)}{\partial x^2}u^2, \quad (28)$$

where u and a are the travelling velocity and acceleration of the vehicle respectively. Similarly, $\dot{Z}_{ri}$ and $\ddot{Z}_{ri}$ can be computed in terms of the relevant degrees of freedom of the bridge and the road surface roughness.

If the ith left and right tyres of the vehicle have not yet entered onto the bridge or they have already left the bridge, these tyres are actually running on the ground. In this case, the vertical displacement, velocity, and acceleration of the ith left contact point, for example, should be determined by the following equations rather than equations (25)–(28).

$$Z_{li} = r_{li}(x), \qquad \dot{Z}_{li} = \frac{\partial r_{li}(x)}{\partial x}\, u, \qquad \ddot{Z}_{li} = \frac{\partial r_{li}(x)}{\partial x}\, a + \frac{\partial^2 r_{li}(x)}{\partial x^2}\, u^2. \tag{29–31}$$

The vertical displacement, velocity, and acceleration of the ith right contact point on the ground should also be computed in a similar way without a direct interaction with the bridge. Now, assume that all the displacements and rotations remain small throughout the analysis. The virtual work done by all the inertial forces, damping forces, and elastic forces acting on the vehicle at a given time can be expressed as

$$\delta W_{VI} = \sum_{i=1}^{3} (\delta Z_{vi} M_{vi} \ddot{Z}_{vi} + \delta\theta_{vi} J_{yvi} \ddot{\theta}_{vi} + \delta\phi_{vi} J_{xvi} \ddot{\phi}_{vi}) + \sum_{i=1}^{5} (\delta Z_{sli} M_{sli} \ddot{Z}_{sli} + \delta Z_{sri} M_{sri} \ddot{Z}_{sri}), \tag{32}$$

$$\delta W_{VD} = \sum_{i=1}^{5} (\delta \Delta_{uli} C_{ui} \dot{\Delta}_{uli} + \delta \Delta_{uri} C_{ui} \dot{\Delta}_{uri} + \delta \Delta_{lli} C_{li} \dot{\Delta}_{lli} + \delta \Delta_{lri} C_{li} \dot{\Delta}_{lri}), \tag{33}$$

$$\delta W_{VE} = \sum_{i=1}^{5} (\delta \Delta_{uli} K_{ui} \Delta_{uli} + \delta \Delta_{uri} K_{ui} \Delta_{uri} + \delta \Delta_{lli} K_{li} \Delta_{lli} + \delta \Delta_{lri} K_{li} \Delta_{lri}), \tag{34}$$

where M_{v1}, M_{v2}, and M_{v3} are the lump mass of the tractor and two trailers, respectively; M_{sli} and M_{sri} $(i = 1, 2, \ldots, 5)$ are the left and right lump mass of the five axle sets, respectively; J_{yv1}, J_{yv2}, and J_{yv3} are the pitching moments of inertia of the tractor and two trailers, respectively; and J_{xv1}, J_{xv2}, and J_{xv3} are the rolling moments of inertia of the tractor and two trailers respectively.

Since there are no masses at the contact points, the matrix $[M_{bbv}]$ and the force vector $\{P_{bvr1}\}$ in equation (7) are zero and the expansion of equation (32) leads to the matrix $[M_v]$. The expansion of the first two terms in equation (34) generates the stiffness matrix $[K_{v1}]$ while the expansion of the last two terms in equation (34) leads to the stiffness matrices $[K_{v2}]$, $[K_{bv}]$, $[K_{vb}]$, $[K_{bbv}]$, the additional force vector $\{P_{vvr3}\}$ on the vehicle, and the additional force vector $\{P_{bvr3}\}$ on the bridge. Similarly, the expansion of equation (33) produces the damping matrices $[C_{v1}]$, $[C_{v2}]$, $[C_{bbv}]$, $[C_{bv}]$, $[C_{vb}]$, and the additional force vectors $\{P_{vvr2}\}$ and $\{P_{bvr2}\}$. For the vehicle–bridge system concerned, the 10 external forces on the bridge (or on the ground) due to the gravity forces of the vehicle should be considered. The virtual work done by all the external forces at a given time can be computed by

$$\delta W_{bp} = \sum_{i=1}^{5} (\delta Z_{li} P_{li} + \delta Z_{ri} P_{ri}), \tag{35}$$

where P_{li} and P_{ri} $(i = 1, 2, \ldots, 5)$ are the 10 external forces on the bridge (or on the ground) at the contact points on the left side and right side, respectively, due to the gravity of the vehicle. The expansion of equation (35) will lead to the force vector $\{P_{bvg}\}$on the bridge (or on the ground). Finally, the computer program will provide the equations of motion of the coupled cable-stayed bridge and vehicle system at a given time as

$$\begin{bmatrix} M_b & 0 \\ 0 & M_v \end{bmatrix} \begin{Bmatrix} \ddot{v}_b \\ \ddot{v}_v \end{Bmatrix} + \begin{bmatrix} C_b + C_{bbv} & C_{bv} \\ C_{vb} & C_{v1} + C_{v2} \end{bmatrix} \begin{Bmatrix} \dot{v}_b \\ \dot{v}_v \end{Bmatrix} + \begin{bmatrix} K_b + K_{bbv} & K_{bv} \\ K_{vb} & K_{v1} + K_{v2} \end{bmatrix} \begin{Bmatrix} v_b \\ v_v \end{Bmatrix}$$

$$= \begin{Bmatrix} P_{bvg} + P_{bvr2} + P_{bvr3} \\ P_{vvr2} + P_{vvr3} \end{Bmatrix}. \tag{36}$$

By using the fully computerized approach, it is very convenient to manage the case in which some or all tyres of a vehicle are not running on the bridge. For instance, if the ith left and right tyres of the investigated vehicle are running on the ground rather than on the bridge deck at a given time, their vertical displacements, velocities, and accelerations will be automatically computed according to equations (29)–(31) rather than equations (25)–(28). This change results in the change in the computation of the virtual work done by damping forces, elastic forces, and external forces in terms of Z_{li}, Z_{ri}, Δ_{lli}, Δ_{lri}, $\dot{\Delta}_{lli}$, and $\dot{\Delta}_{lri}$ in equations (33)–(35). The virtual work done by inertia forces has no change in this case study because there are no masses at contact points. Consequently, the expansion of the virtual work done by the damping forces, elastic forces, and external forces lead to the change in the sub-damping matrices $[C_{bbv}]$, $[C_{bv}]$, $[C_{vb}]$, the sub-stiffness matrices $[K_{bbv}]$, $[K_{bv}]$, $[K_{vb}]$, and the sub-sub loading vector $\{P_{bvg}\}$ in equation (36). All these will be done by the computer automatically.

4.4. ROAD SURFACE ROUGHNESS

In this case study, the value of roughness coefficient A_r in equation (5) is taken as 20×10^{-6} m^3/cycle according to International Organisation for Standardisation (ISO) specification [18] for good road. The sample length is taken as 2048 m. A total of 16 384 (2^{14}) data points are generated within the length. The vertical road surface profile averaged from five simulations for good road is shown in Figure 4 and used for later presentation.

4.5. SOLUTION OF EQUATIONS OF MOTION

This case study considers the five identical tractor–trailer vehicles arranged in line at interval of 10 m. The equations of motion achieved are a set of coupled second order

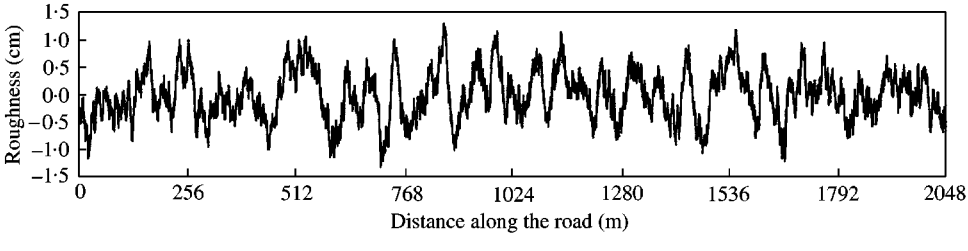

Figure 4. Vertical good road surface profile.

differential equations with time-varying coefficients. The total degrees of freedom of the five vehicles are 85 with each vehicle assembled in the same way as described in section 4.3. The Wilson–θ method is used in this study for determining dynamic responses of both vehicle and bridge. The θ value and the time interval used in the computation are 1·4 and 0·02 s respectively.

4.6. MAJOR RESULTS

4.6.1. *Response of bridge*

Displayed in Figures 5(a) and 6(a) are the time histories of the vertical displacement responses of the bridge at points A and B respectively, when the five heavy road vehicles arranged in line at interval of 10 m run on lane 2 of the bridge at a constant velocity of 40 km/h. Point A is located at the middle point of the middle section of the left main span while point B is situated at the middle point of the middle section of the right main span (see Figures 1 and 2). Lane 2 is the middle lane of the left three-lane carriageway (see Figure 2). It is seen from Figures 5(a) and 6(a) that the vertical displacements of the bridge are quite small when the vehicles run on the left- and right-side spans. The maximum vertical displacement response at each point occurs almost when the vehicles run around that point. The pattern of the displacement response, however, depends on the position concerned. For instance, it is seen from the displacement response of bridge at point A that when the vehicles travel on the left side span, the bridge response at point A is quite small. When the vehicles travel on the left main span, the bridge response becomes large and downward. As the vehicles travel on the right main span, the displacement response becomes upward. Although the maximum vertical displacement response of the bridge at point A reaches 0·279 m, it is very small compared with the left main span of 448 m. This may be because the bridge is a low-frequency system, of which the lowest vertical natural frequency is 0·189 Hz while the vehicle is a high-frequency system of which the lowest vertical nature frequency is 3·21 Hz. Also, because the bridge is relatively long and heavy and the vehicles are relatively small and light, the vertical dynamic displacement response looks like the static influence line.

Figures 5(b) and 6(b) show the time histories of the vertical acceleration responses of the bridge at points A and B respectively. It is seen that when the vehicles travel around the

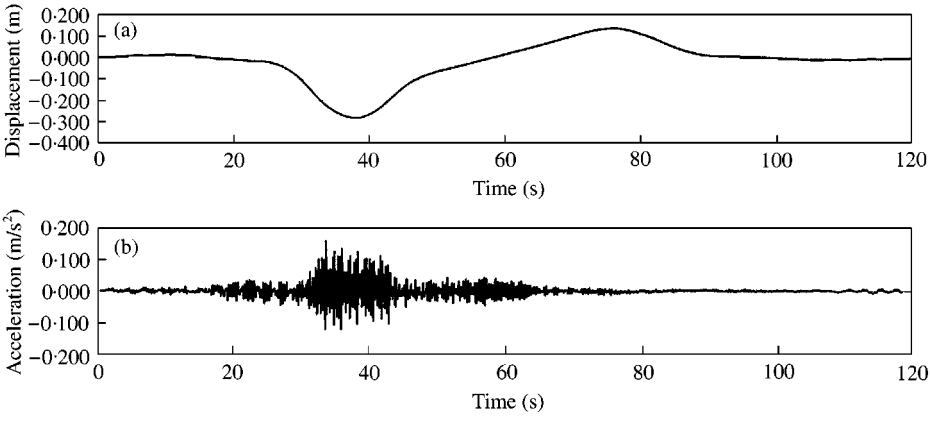

Figure 5. Vertical dynamic response of bridge at point A ($u = 40$ km/h): (a) vertical displacement response; (b) vertical acceleration response.

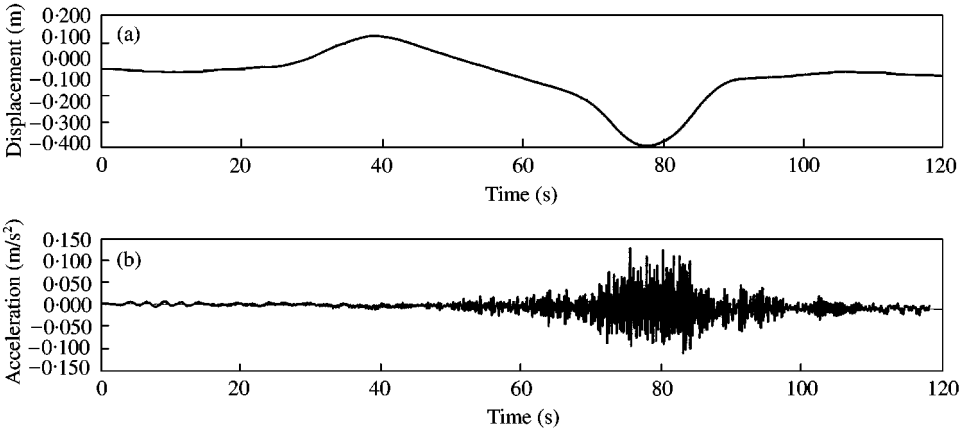

Figure 6. Vertical dynamic response of bridge at point B ($u = 40$ km/h): (a) vertical displacement response; (b) vertical acceleration response.

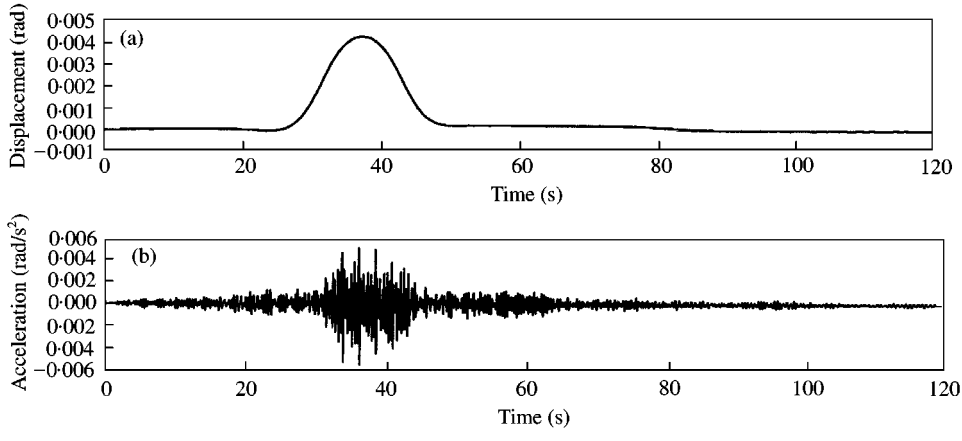

Figure 7. Torsional dynamic response of bridge of section A ($u = 40$ km/h): (a) torsional displacement response; (b) torsional acceleration response.

points concerned, the bridge vertical acceleration responses at the points are quite large. When the vehicles travel far from the points concerned, the bridge vertical acceleration responses at the two points become quite small. This indicates that the bridge acceleration response due to vehicles is localized.

Displayed in Figures 7 and 8 are the time histories of the torsional displacement and acceleration responses of the bridge at sections A and B respectively. It is seen that when the vehicles travel around the sections concerned, the bridge torsional displacement and acceleration responses at the sections become relatively large. The bridge torsional displacements are almost positive in the anticlockwise direction because the vehicles travel on the left carriageway. The bridge torsional displacement and acceleration responses are quite small, which indicates that the bridge deck supported by the four planes of stay cables can take action well under the eccentric traffic load.

The bridge responses at points A and B are also computed for the vehicles running at different speed. The maximum vertical and torsional displacement and acceleration

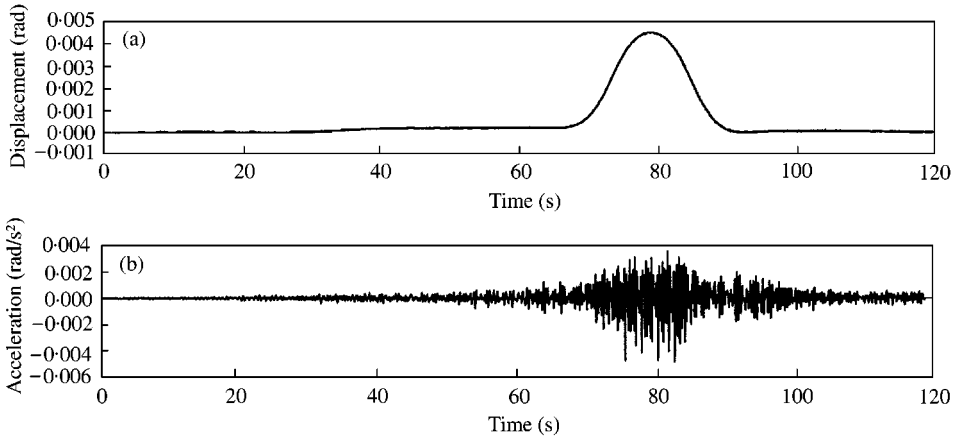

Figure 8. Torsional dynamic response of bridge of section B ($u = 40$ km/h): (a) torsional displacement response; (b) torsional acceleration response.

TABLE 2

Maximum responses of bridge and vehicles[†]

Type of responses	Unit	$u = 40$ km/h	$u = 60$ km/h	$u = 80$ km/h
Deck vertical displacement	m	0·281	0·289	0·292
Deck vertical acceleration	m/s^2	0·162	0·310	0·176
Deck torsional displacement	rad	0·00447	0·00451	0·00452
Deck torsional acceleration	rad/s^2	0·00544	0·0104	0·00575
Vehicle vertical displacement	m	0·218	0·216	0·221
Vehicle vertical acceleration	m/s^2	3·117	4·455	5·216

[†]*Note*: u is the vehicle speed.

responses of the bridge at the two positions are listed in Table 2. It is seen that the maximum vertical displacement responses increase slightly with increasing vehicle speed. However, the maximum vertical acceleration responses occur at the vehicle speed of 60 km/h. The reason why the vertical acceleration response of the bridge is larger at the vehicle speed of 60 m/s than at the vehicle speed of 80 m/s may be due to the resonance and cancellation phenomena, as discussed by Yang *et al.* [19]. However, further investigation should be carried out on this point because the coupled vehicle–bridge system considered in this paper is too complicated.

The dynamic impact factor for the vertical displacement of the bridge subjected to the moving vehicles is defined as

$$I = \frac{R_d(x) - R_s(x)}{R_s(x)}, \tag{37}$$

where $R_d(x)$ and $R_s(x)$ denote, respectively, the maximum dynamic and static vertical displacement responses of the bridge at point x due to the moving vehicles. The computation results show that the maximum dynamic and static vertical displacement responses of the bridge occur at point B for all the concerned vehicle speeds. The corresponding dynamic impact factors are 0·0203, 0·0482, and 0·0595 for the vehicle speed of

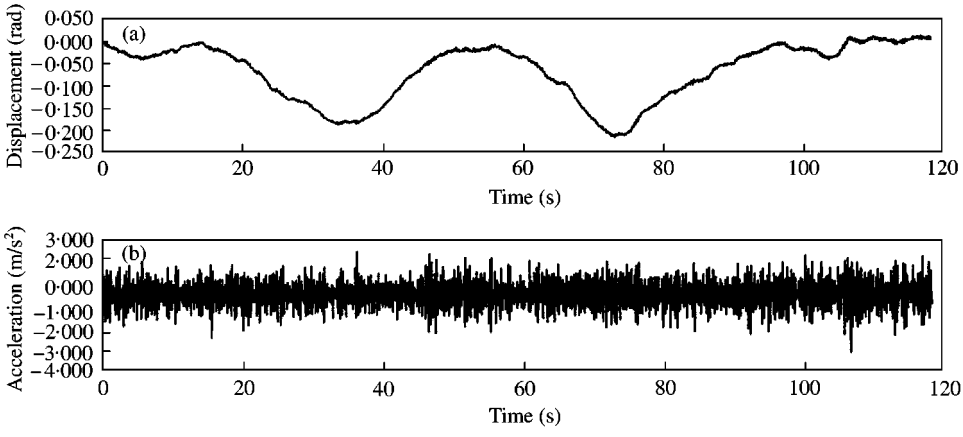

Figure 9. Vertical dynamic response of the tractor of the first vehicle ($u = 40$ km/h): (a) vertical displacement response; (b) vertical acceleration response.

40, 60, and 80 km/h respectively. These dynamic impact factors indicate that the dynamic effects of the moving vehicles are insignificant.

4.6.2. *Response of vehicles*

Displayed in Figure 9(a) is the time history of the vertical displacement response of the tractor of the first vehicle that runs on the bridge deck at a constant speed of 40 km/h. It is seen that when the vehicles travel on the left- or right-side spans, the vertical displacement of the vehicle is relatively small. When the vehicles travel on the left or right main spans, the vertical displacement of the vehicle becomes relatively large. This is because the vertical displacement of the vehicle depends on the relevant displacement of the bridge deck on which the vehicle runs.

Displayed in Figure 9(b) is the time history of the vertical acceleration response of the tractor of the first vehicle, which may serve as an indicator of the driver and passenger comfort. It is seen that the amplitude of vertical acceleration response of the vehicle remains almost the same no matter where the vehicle runs, the side span or the main span. Obviously, the vertical acceleration response of the vehicle contains much higher-frequency component than the vertical displacement response of the vehicle. The results listed in Table 2 also show that the maximum acceleration response of the vehicle increases with the increasing vehicle speed while the maximum displacement response of the vehicle varies a little with increasing vehicle speed.

5. CONCLUSIONS

A fully computerized approach for assembling equations of motion of any types of coupled vehicle–bridge systems and for investigating vehicle–bridge interaction has been proposed in this study. The implementation of the computerized approach in the computer program with road surface roughness included has been introduced in detail. The computerized approach and the associated computer program were then applied to a real long span cable-stayed bridge with a group of five moving heavy road vehicles arranged in line at a certain interval. It was demonstrated that the fully computerized approach provided an efficient and convenient tool for studying the interaction problems of large

complicated bridges under various types of vehicles. The fully computerized approach could well predict dynamic behaviours of both bridge and vehicles with reasonable computation efforts.

ACKNOWLEDGMENTS

The writers are grateful for the financial support from the Research Grants Council of Hong Kong through a RGC research grant (5027/98E) for the second writer and a Postgraduate Scholarship from Drs Richard Charles & Esther Yewpick Lee Charitable Foundation to the first writer.

REFERENCES

1. T. E. BLEJWAS, C. C. FENG, and R. S. AYRE 1979 *Journal of Sound and Vibration* **67**, 513–521. Dynamic interaction of moving vehicles and structures.
2. M. OLSSON 1985 *Journal of Sound and Vibration* **99**, 1–12. Finite element modal co-ordinate analysis of structures subjected to moving loads.
3. M. F. GREEN, D. CEBON and D. J. COLE 1995 *Journal of Structural Engineering American Society of Civil Engineers* **121**, 272–282. Effects of vehicle suspension design on dynamics of highway bridges.
4. T. L. WANG, D. Z. HUANG and M. SHAHAWY 1996 *Journal of Bridge Engineering American Society of Civil Engineers* **1**, 67–75. Dynamic behavior of continuous and cantilever thin-walled box girder bridges.
5. Y. K. CHEUNG, F. T. K. AU, D. Y. ZHENG and Y. S. CHENG 1999 *Journal of Sound and Vibration* **228**, 611–628. Vibration of multi-span non-uniform bridges under moving vehicles and trains by using modified beam vibration functions.
6. S. TIMOSHENKO, D. H. YOUNG and W. WEAVER 1974 *Vibration Problems in Engineering*. New York: Wiley, fourth edition.
7. E. S. HWANG and A. S. NOWAK 1991 *Journal of Structural Engineering American Society of Civil Engineers* **117**, 1413–1434. Simulation of dynamic for bridges.
8. Y. B. YANG and J. D. YAU 1997 *Journal of Structural Engineering American Society of Civil Engineers* **123**, 1512–1518. Vehicle–bridge interaction element for dynamic analysis.
9. K. HENCHI, M. FAFARD, M. TALBOT and G. DHATT 1998 *Journal of Sound and Vibration* **212**, 663–683. An efficient algorithm for dynamic analysis of bridges under moving vehicles using a coupled modal and physical components approach.
10. Y. B. YANG and H. B. LIN 1995 *Journal of Structural Engineering American Society of Civil Engineers* **121**, 1636–1643. Vehicle-bridge interaction analysis by dynamic condensation method.
11. Y. L. XU, J. M. KO and W. S. ZHANG 1997 *Journal of Bridge Engineering American Society of Civil Engineers* **2**, 149–156. Vibration studies of Tsing Ma suspension bridge.
12. T. L. WANG and D. Z. HUANG 1992 *Journal of Structural Engineering American Society of Civil Engineers* **118**, 1354–1374. Cable-stayed bridge vibration due to road surface roughness.
13. C. J. DODDS and J. D. ROBSON 1973 *Journal of Sound and Vibration* **31**, 175–183. The description of road surface roughness.
14. D. Z. HUANG and T. L. WANG 1992 *Computers and Structures* **43**, 897–908. Impact analysis of cable-stayed bridges.
15. W. H. GUO and Y. L. XU 2000 *Proceedings of International Conference on Advances in Structural Dynamics, Hong Kong*, Vol. I, 513–520. Direct assembling matrix method for dynamic analysis of coupled vehicle–bridge systems.
16. L. D. ZHU, H. F. XIANG and Y. L. XU 2000 *Engineering Structures* **22**, 1313–1323. Triple-girder model analysis of cable-stayed bridges with warping effect.
17. M. FAFARD, M. BENNUR and M. SAVARD 1997 *Engineering Computations* **14**, 491–508. A general multi-axle vehicle model to study the bridge–vehicle interaction.
18. C. J. DODDS 1972 *International Organization for Standardisation ISO/TC*/108/*WG*9, *Document No.* 5. BSI proposals for generalised terrain dynamic inputs to vehicles.
19. Y. B. YANG, J. D. YAU and L. C. HSU 1997 *Engineering Structures* **19**, 936–944. Vibration of simple beams due to trains moving at high speeds.